

Assessment and Analysis of Gas Flow Temperature in Gas Production: A Case Study in VietNam

Ta Quoc Dung^{1,2,*}, Do Duc Anh^{1,2}



Use your smartphone to scan this QR code and download this article

ABSTRACT

In this study, a comprehensive model is introduced for predicting fluid flow temperature in gas wells, integrating the mechanical energy balance equation with convection, conduction, and radiation modes of heat transfer. The pressure calculation process is enhanced by the incorporation of the Gray correlation. The key findings reveal a remarkable consistency between the proposed model and measured data, demonstrating deviations of only 0.34% and 0.63% for pressure loss prediction and temperature distribution along the borehole, respectively. Nodal analysis emerges as a valuable technique, enabling precise calculations of pressure and temperature in the wellbore and reservoir flow. Through sensitivity analysis, the study evaluates the impact of various factors, such as tubing size and production rate, on temperature and pressure in the wellbore, considering both wellhead and bottom hole locations. Conclusions drawn from the sensitivity analysis underscore the significant influence of changes in flow rate on temperature along the production tubing, with an increase from 20 to 100 mmscf/d resulting in a temperature rise from 150 to 300 °F. Tubing size is identified as a crucial determinant in pressure loss calculations, showing a slight decrease in wellhead temperature from 281 to 252 °F when increasing tubing size from 3 to 5.5 inches at a fixed production rate. However, variations in tubing diameter exhibit substantial effects on temperature and pressure under different operating production rates.

Key words: Temperature, Pressure, Nodal Analysis, Temperature Model, Gas Well Deliverability

¹Faculty of Geology and Petroleum, Ho Chi Minh City University of Technology (HCMUT), Ho Chi Minh City, Vietnam

²Vietnam National University Ho Chi Minh City, Vietnam

Correspondence

Ta Quoc Dung, Faculty of Geology and Petroleum, Ho Chi Minh City University of Technology (HCMUT), Ho Chi Minh City, Vietnam

Vietnam National University Ho Chi Minh City, Vietnam

Email: tqdung@hcmut.edu.vn

History

- Received: 18-10-2023
- Accepted: 05-3-2024
- Published Online:

DOI :



Copyright

© VNUHCM Press. This is an open-access article distributed under the terms of the Creative Commons Attribution 4.0 International license.



INTRODUCTION

The control of production pressure within the production tubing is integral to facilitating upward flow during the production process. Concurrently, temperature regulation is crucial for managing the production volume. Elevated pressure and reduced temperature conditions can induce two-phase flow, resulting in substantial damage to the system. While temperature variations during gas flow may not directly influence pressure data, they do impact parameters like the Z factor and gas viscosity, thereby introducing errors in pressure calculations. Consequently, there has been a notable focus on studying temperature changes within the production tubing of gas wells. Alves et al. (1992)¹ underscored those prior correlations developed by researchers aimed at simplifying calculations often yielded unrealistic estimations for more general scenarios. To address this limitation, they proposed a method that incorporates fewer restrictive assumptions. Their approach is applicable to pipelines, production, and injection wells, accommodating single- or two-phase flow, and encompassing a broad range of inclination angles from horizontal to vertical, utilizing both compositional and black-oil fluid models.

This research centers on examining the temperature model of well WELL 1X in the BlackCat gas field, situated in the Cuu Long basin, Vietnam. To achieve a more comprehensive computation of fluid temperature distribution within the production pipe for deep water production, an analysis model introduced by Alves et al. is employed. Additionally, Gray correlation is utilized to estimate pressure losses throughout the wellbore. Subsequently, a production evaluation and well performance analysis, employing Nodal Analysis, are conducted, considering various changes in tubing size and flow rate^{2,3}.

By employing these methodologies and techniques, a more precise understanding of the temperature profile and its impact on overall well performance can be achieved, particularly in the context of deep-water production scenarios in the BlackCat gas field⁴.

METHODOLOGY

Heat transfer mechanism

Figure 1 shows the thermal exchange between hydrocarbon fluid and the inner wall of the tubing predominantly transpires through forced convection. Furthermore, heat is conducted through the tubing wall, casing wall, and the cement sheath⁴. Within the annular

Cite this article : Dung T Q, Anh D D. **Assessment and Analysis of Gas Flow Temperature in Gas Production: A Case Study in VietNam.** *Sci. Tech. Dev. J. – Engineering and Technology* 2024; ():1-10.

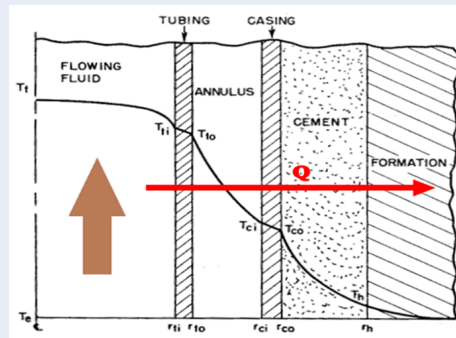


Figure 1: Wellbore heat transfer and temperature distribution⁵

50 space, conventionally occupied by completion fluids
 51 between the casing and tubing, heat transfer involves
 52 contributions from both radiation and natural convec-
 53 tion. This section will intricately explore the partic-
 54 ulars of each mechanism of heat loss from the fluid
 55 to the surrounding formation, drawing upon insights
 56 elucidated in the work of Willhite (1967)⁶.

57 **Heat conductive transfer**

58 The heat transfer arising from conduction can be
 59 characterized using Fourier’s equation in radial coordi-
 60 nates. A visual representation of the conduction-
 61 based heat transfer is depicted in Figure 2, as outlined
 62 in the work of reference⁵.

$$Q = 2\pi r \Delta L k \frac{\partial T}{\partial r} \tag{1}$$

63 By taking the integration of (1), heat transfer is ex-
 64 pressed:

$$Q = \frac{2\pi k (T_i - T_o) \Delta L}{\ln\left(\frac{r_o}{r_i}\right)} \tag{2}$$

65 Due to the elevated thermal conductivity and the rel-
 66 atively diminutive radial separation between flowing
 67 fluids and the borehole wall, heat transfer in the ad-
 68 jacent walls is typically regarded as being in a steady
 69 state⁷.

$$Q = \frac{(2\pi k_t (T_{ti} - T_{to}) \Delta L)}{\ln\left(\frac{r_{to}}{r_{ti}}\right)} \tag{3}$$

70 Casing wall:

$$Q = \frac{(2\pi k_{ca} (T_{ci} - T_{co}) \Delta L)}{\ln\left(\frac{r_{co}}{r_{ci}}\right)} \tag{4}$$

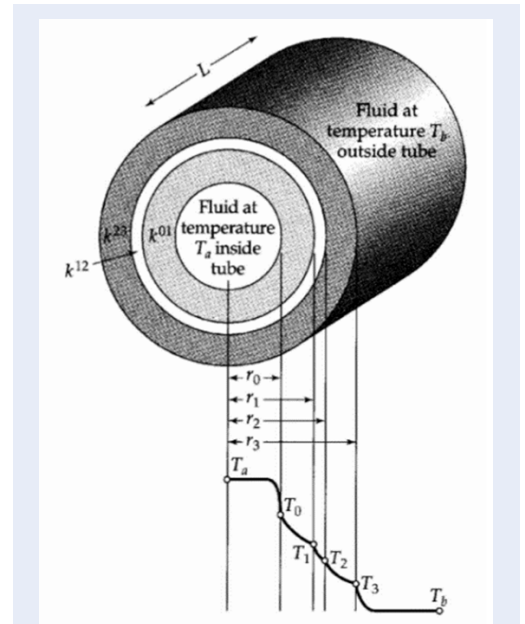


Figure 2: Heat conduction through cylindrical tubing⁵

Cement sheath:

$$Q = \frac{2\pi k_{cement} (T_{co} - T_h) \Delta L}{\ln\left(\frac{r_b}{r_{co}}\right)} \tag{5}$$

72 The conveyance of heat into the adjacent rock trans-
 73 pires via heat conduction, constituting a transient
 74 process. Given the typically substantial volume of
 75 rock, approaching infinity, the attainment of steady-
 76 state conditions in this context may extend over peri-
 77 ods of several months or even years. The transient
 78 radial heat conduction equation is employed to artic-
 79 ulate this process and is formulated as follows:

$$Q = \frac{2\pi k_e (T_h - T_e) \Delta L}{f(t)} \tag{6}$$

80 The determination of the dimensionless time function
 81 can be ascertained through the work of Hasan and
 82 Kabir⁵.

$$f(t) = 1.1281\sqrt{t_D} [1 - 0.3\sqrt{t_D}] \quad (t_D \leq 1.5) \tag{7}$$

$$f(t) = [0.4063 + 0.5 \ln(t_D)] \left[1 + \frac{0.6}{t_D} \right] \quad (t_D > 1.5) \tag{8}$$

83 **Convective and Radiative heat transfer**

84 **Annulus fluid**

85 The expression for radial heat due to natural convec-
86 tion and radiation of the fluid within the annulus is
87 articulated as follows:

$$Q = 2\pi r_{ci} (h_{c,an} + h_{r,an}) (T_{to} - T_{ci}) \Delta L \quad (9)$$

88 The suggested correlation for the estimation of the
89 convective heat coefficient within the annulus is pre-
90 sented by Dropkin and Sommerscales. The formula
91 they propose is as follows:

$$h_{c,an} = \frac{0.049 (GrPr)^{\frac{1}{3}} Pr^{0.074} k_{an}}{r_{to} \ln \left(\frac{r_{ci}}{r_{to}} \right)} \quad (10)$$

92 The flow regime in natural convection is determined
93 by the dimensionless Grashof number, expressed as
94 follows:

$$Gr = \frac{g \rho_{an}^2 \beta (T_{to} - T_{ci}) (r_{ci} - r_{to})^3}{\mu_{an}^2} \quad (11)$$

95 The Prandtl number in equation (10) can be defined
96 as follows::

$$Pr = \frac{\mu_{an} c_{pan}}{k_{an}} \quad (12)$$

97 The calculation of the heat transfer coefficient for ra-
98 diation within the annulus can be derived using the
99 Stefan-Boltzmann law applied to a concentric annu-
100 lus:

$$h_{r,an} = \frac{\sigma (T_{to}^2 + T_{ci}^2) (T_{to} + T_{ci})}{\frac{1}{r_{to}} + \frac{r_{to}}{r_{ci}} \left(\frac{1}{r_{to}} - 1 \right)} \quad (13)$$

101 Tubing fluid

102 The expression for radial heat due to forced convec-
103 tion within the tubing is as follows:

$$Q = 2\pi r_{ti} h_{c,f} (T_f - T_{ti}) \Delta L \quad (14)$$

104 $h_{c,f}$ These mathematical expressions can be utilized
105 for the calculation:

$$h_{c,f} = \frac{k_f}{2r_{ti}} Nu \quad (15)$$

$$Nu = 0.023 (Re)^{0.8} (Pr)^{\frac{1}{3}} \quad (16)$$

106 The Prandtl number, denoted as Pr, can be deter-
107 mined by substituting the relevant properties of the
108 tubing fluid into equation (12).

Overall Heat Transfer Coefficient

110 The radial heat transfer transpires between the well-
111 bore fluid and the formation, surmounting various re-
112 sistances as illustrated in Figure 1. This process can be
113 expressed as follows:

$$Q = 2\pi r_{to} U_{to} (T_f - T_h) \Delta L \quad (17)$$

114 As previously mentioned, the limited radial separa-
115 tion between the flowing fluids and the borehole wall
116 typically renders the heat transfer process as steady
117 state. Consequently, the heat flowing through each
118 element illustrated in Figure 1 is equalized. Through
119 this analysis, the combination of equations (3), (4),
120 (5), (9), and (14) yields the comprehensive heat trans-
121 fer equation.

$$U_{to} = r_{to}^{-1} \left[\frac{1}{r_{ti} h_{c,f}} + \frac{\ln \left(\frac{r_{to}}{r_{ti}} \right)}{k_t} + \frac{1}{r_{ci} (h_{c,an} + h_{r,an})} + \frac{\ln \left(\frac{r_{co}}{r_{ci}} \right)}{k_c} + \frac{\ln \left(\frac{r_h}{r_{co}} \right)}{k_{cement}} \right]^{-1} \quad (18)$$

122 Several acceptable assumptions can be made to sim-
123 plify equation (18). The high heat transfer coefficient
124 of the fluid results in T_f being approximately equal to
125 T_{ti} . Additionally, the substantial thermal conductiv-
126 ity of metals, along with the relatively thin tubing and
127 casing walls, permits the neglect of resistances asso-
128 ciated with these elements. Consequently, equation
129 (18) can be simplified to:

$$U_{to} = r_{to}^{-1} \left[\frac{1}{r_{ci} (h_{c,an} + h_{r,an})} + \frac{\ln \left(\frac{T_h}{T_{co}} \right)}{k_{cement}} \right]^{-1} \quad (19)$$

Temperature Model

130 The derived equation for the temperature profile is
131 founded on the principles of mass conservation, momen-
132 tum, and energy balance within a differential
133 control volume of a pipe. The temperature formula-
134 tion proposed by Alves et al.¹ can be represented as
135 follows:
136

$$\frac{dT_f}{dL} = -\frac{(T_f - T_c)}{A} - \frac{g \cos(\theta)}{c_p g_c j} - \phi \quad (20)$$

$$A = \frac{c_p w}{U_{to} \pi r_{to}} \quad (21)$$

$$\phi = \frac{v}{c_p g_c j} \frac{dv}{dL} - \eta \frac{dP}{dL} \quad (22)$$

137 **Pressure-gradient calculating for gas well**
 138 **performance.**

139 The equation describing the pressure gradient for gas
 140 flow within a pipe is conventionally articulated to rep-
 141 resent the total pressure loss^{5,6}.

$$\frac{dp}{dz} = \frac{f\rho_n v_m^2}{2d} + \frac{g_c}{g} \rho_s \sin(\theta) \quad (24)$$

- 142 f: friction number.
- 143 d: tubing inside diameter, ft.
- 144 ρ_n : mixture average density of liquid and gas phase,
 145 lbm/ft³
- 146 ρ_s : slip mixture density of liquid and gas phase
 147 lbm/ft³.
- 148 v_m : mixture average velocity, ft/sec.

149 **Nodal analysis**

150 Nodal analysis constitutes a systematic methodology
 151 employed in the optimization of oil and gas wells. This
 152 approach entails a thorough examination of the entire
 153 producing system, allowing for a meticulous evalua-
 154 tion of each component. Whether applied to individ-
 155 ual components within a producing well or multiple
 156 wells within a production system, nodal analysis seeks
 157 to optimize these elements to attain the desired flow
 158 rate. Through the consideration of the characteristics
 159 and interactions of various components in the system,
 160 nodal analysis facilitates the identification of oppor-
 161 tunities for improvement and the implementation of
 162 effective optimization strategies⁸.

163 In the analysis of the production system, a compre-
 164 hensive consideration of all pertinent components is
 165 undertaken, commencing from the static reservoir
 166 pressure, and extending to the separator. Figure 3
 167 delineates a production system, emphasizing distinct
 168 nodes within the red circle, and provides estimations
 169 of pressure losses for each component. The central
 170 focus of this investigation revolves primarily around
 171 wellbore nodal analysis, an approach that amalga-
 172 mates reservoir inflow and wellbore lift capabilities.
 173 This integration is achieved by intersecting the Inflow
 174 Performance Relationship (IPR) and Tubing Perfor-
 175 mance Relationship (TPR) curves on a pressure and
 176 production rate plot, facilitating the prognostication
 177 of operating flow rates⁹.

178 Moreover, sensitivity evaluations are conducted to
 179 optimize production or identify potential issues by
 180 scrutinizing the effects of varying parameters.

181 **Inflow Performance:**

182 The Inflow Performance Relationship (IPR) elucidates
 183 the correlation between the producing bottomhole
 184 pressures of a well and the corresponding production

185 rates, under a specified reservoir condition. It offers
 186 insights into how the well's productivity varies with
 187 changing bottomhole pressures³.

188 **Tubing Performance:**

189 The Tubing Performance Relationship (TPR) delin-
 190 eates the fluid's performance as it traverses through
 191 the tubing in the borehole⁸. This relationship gen-
 192 erates a plot of the bottomhole pressure against the
 193 corresponding flow rate. In constructing this perfor-
 194 mance model, it is imperative to account for varia-
 195 tions in pressure and temperature to maintain a sta-
 196 ble flow rate. Given the consequential alterations in
 197 the flow's independent properties, the black oil model
 198 emerges as a valuable tool in addressing this issue and
 199 faithfully representing the fluid's behavior in the well-
 200 bore⁸.

201 **RESULTS AND DISCUSSION**

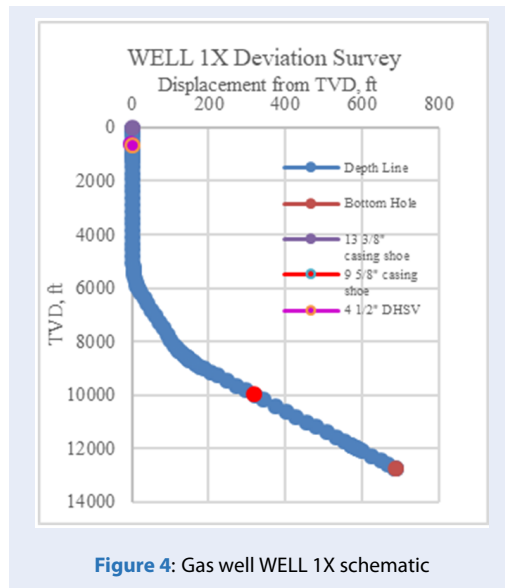
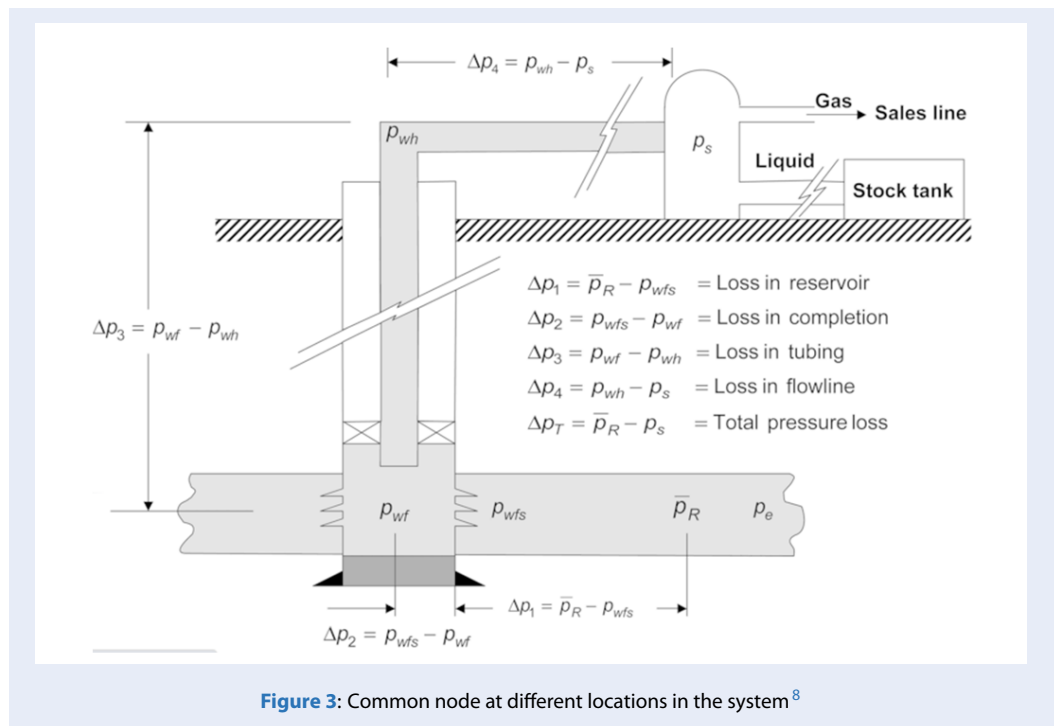
202 In this section, the veracity of the proposed method-
 203 ology is substantiated through a comparative analysis
 204 between the predicted model and actual field data ac-
 205 quired from gas well WELL 1X in the BlackCat gas
 206 field. The assessment of vertical lift performance is
 207 conducted by employing the Gray correlation with the
 208 Prosper software, which facilitates the derivation of a
 209 comparable result for the operating point in contrast
 210 to the curve derived using a temperature model. This
 211 comparative analysis serves to evaluate the precision
 212 and efficacy of the proposed approach. Furthermore,
 213 sensitivity studies will be undertaken to scrutinize the
 214 ramifications of variations in parameters on the as-
 215 sessment of gas well performance. Through the ex-
 216 ploration of diverse parameter scenarios, a compre-
 217 hensive comprehension of the factors influencing gas
 218 well performance can be attained.

219 **Well data acquisition and analysis**

220 **Well deviation survey**

221 Prior to simulating field cases and conducting sensi-
 222 tivity analyses, data acquisition and analysis represent
 223 pivotal preparatory steps. Figure 4 furnishes a com-
 224 prehensive overview of the well's depth profile, denot-
 225 ing its extension to a total measured depth (MD) of
 226 13,418 ft and a total vertical depth (TVD) of 12,731 ft.
 227 The production tubing encompasses the entire length
 228 of 13,418 ft MD, while the bottom hole registers a ver-
 229 tical depth of 12,731 ft. Positioned at a depth of 659 ft
 230 TVD is a 4 1/2" downhole safety valve located at the
 231 well's summit. The well comprises 13 3/8" and 9 5/8"
 232 casing sections, with shoe locations at 6,662 ft MD and
 233 10,329 ft MD, respectively.

234 Drilled in a vertical orientation from the surface to
 235 a depth of 5,900 ft, the well subsequently transitions



236 into horizontal drilling towards the bottom hole. The
 237 inclination angle fluctuates between 2° and 20° con-
 238 cerning the vertical axis, indicative of the alteration in
 239 drilling direction.
 240 These delineated details furnish the requisite contex-
 241 tual information for the subsequent simulation en-
 242 deavors, field case analyses, and sensitivity assess-
 243 ments pertaining to the well's performance.

Well data input

244 This study examines data extracted from WELL 1X
 245 within the BlackCat gas field, located in Vietnam. The
 246 data comprises various parameters pertaining to the
 247 well's information [Table 1], Fluid data [Table 2] and
 248 Reservoir data [Table 3], as outlined below.
 249

Methodology

250
 251 **Coupling algorithm:** In the coupling algorithm, two
 252 levels of sophistication can be employed when amal-
 253 gamating the heat balance and mechanical energy bal-
 254 ance equations to concurrently compute pressure and
 255 temperature changes². Achieving convergence on
 256 both pressure and temperature within a specified pipe
 257 length increment necessitates the implementation of
 258 a double-iterative procedure, as illustrated in Figure 5.
 259

Temperature profile of gas well WELL 1X

260
 261 In general, a favorable correspondence is observed be-
 262 tween the calculated and measured temperature pro-
 263 files from the wellhead to a depth of 8,000 ft, as illus-
 264 trated in Figure 6. However, discernible discrepan-
 265 cies emerge in the lower section of the well, specifi-
 266 cally spanning from 8,100 ft to the bottom hole, as
 267 depicted in Figure 7. This incongruity can be ascribed
 268 to the presence of downhole equipment influenced by
 269 heat conductive mechanisms, which, if not duly con-
 270 sidered, may introduce errors in the calculations.

Table 1: Well data input data

Well Information		
Well head pressure	1890	psig
Well head temperature	268	oF
CGR	0.0003	bbls/mmscf
Gas flow rate	55.5	MMscf/day

Table 2: Fluid data of gas well WELL 1X

Gas composition (%)			
N2	0.08	iC4	1.32
Co2	0.07	nC4	2.14
H2S	0	iC5	0.91
C1	70.5	nC5	1.01
C2	9.11	nC6	1.3
C3	1.32	C6+	8.23

Table 3: Reservoir data for gas well WELL 1X

Pr (psi)	7500
Tr (°R)	810
Thickness (ft)	300
Permeability (mD)	2
Rw, ft	0.25
Re, ft	2979
Skin factor	2
D, non – Darcy flow factor	0.00006

271 The noted disparities in temperature data under-
 272 score the significance of accounting for the impact
 273 of heat conductive mechanisms on downhole equip-
 274 ment. This underscores the imperative for more pre-
 275 cise models that incorporate these effects, ensuring
 276 enhanced temperature predictions and more depend-
 277 able evaluations of well performance.

278 The fluid temperature is initially determined by the
 279 bottom hole temperature, which is equivalent to the
 280 formation heat as shown in Figure 8. Subsequently,
 281 heat is transferred outward through the annulus and
 282 casing in a horizontal direction, leading to a decrease
 283 in temperature. The annulus fluid is disregarded, and
 284 as air occupies the annulus, which possesses a rela-
 285 tively low thermal conductivity, the heat transfer from
 286 the inside and outside of the casing becomes approx-
 287 imately equal.

Pressure profile of gas well WELL 1X

288 The application of Gray correlation to determine pres-
 289 sure gradients yields highly accurate pressure values
 290 when compared to measured data as shown in Fig-
 291 ure 9. The analysis employed identical temperature
 292 profile values. Conversely, the model lacking a tem-
 293 perature component exhibits a significant deviation
 294 from the measured data, indicating a lack of con-
 295 fidence in its accuracy. In contrast, the tempera-
 296 ture model, which incorporates the pressure model,
 297 closely aligns with the measured data, demonstrat-
 298 ing its reliability. Consequently, this integrated model
 299 can be effectively utilized.
 300

301 The significance of using temperature data to pre-
 302 dict pressure at bottom hole is further emphasized
 303 by the findings in Figure 10 and Table 4. The tem-
 304 perature profile derived from Prosper, which calcu-
 305 lates gas temperature based on surrounding tempera-
 306 ture and utilizes a simple linear interpolation method

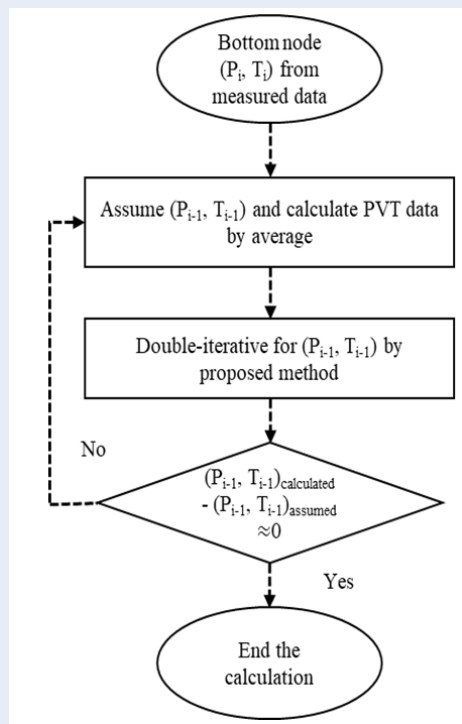


Figure 5: General workflow illustration

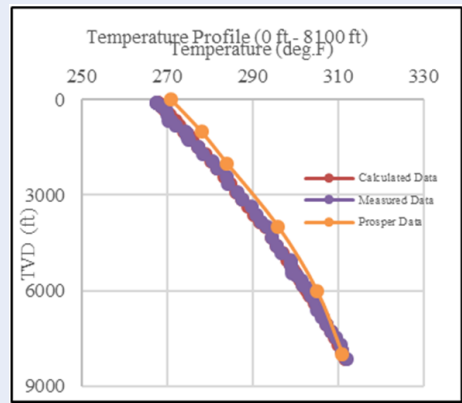


Figure 6: Predicted with Measured temperature (0-8100 ft)

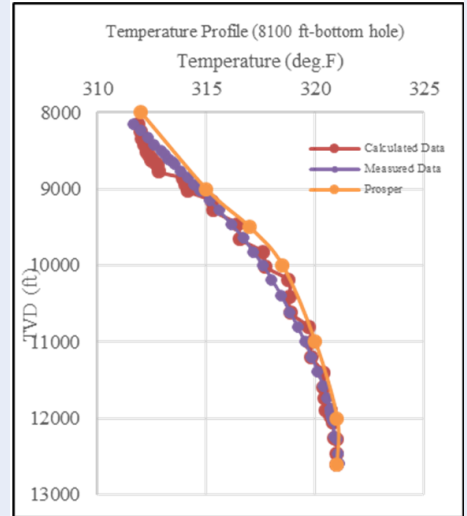


Figure 7: Predicted and Measured temperature (8100 ft-Bottom hole)

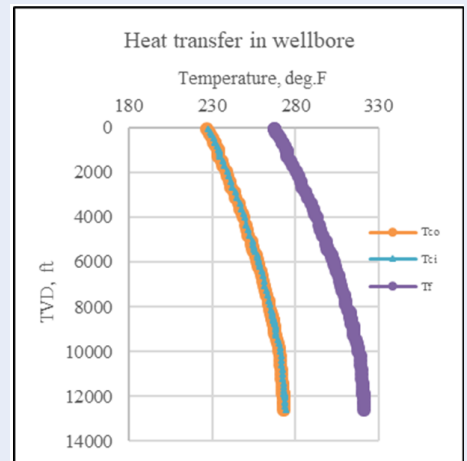


Figure 8: Heat transfer from tubing to casing

307 to compute bottom hole pressure, demonstrates low
 308 accuracy when compared to measured data. Con-
 309 sequently, it is recommended to replace the linear
 310 interpolation approach with a more comprehensive
 311 heat transfer analysis that incorporates relevant heat
 312 mechanisms. This enhancement will lead to improved
 313 accuracy in temperature predictions and subsequent
 314 pressure calculations.

Sensitivity analysis

**Effect of gas flow rate on the wellhead tem-
 perature.**

In any production scenario, it is imperative for the
 wellhead temperature to be lower than that at the
 bottom hole. Referring to Figure 11, if the bottom
 hole temperature is maintained at a constant value of
 321°F, with a gas production rate of 55 mmscf/day, the
 wellhead temperature is calculated to be 268°F. This
 observation suggests that when gas flows rapidly to
 the wellhead, temperature loss is minimized due to
 the limited convection within the production tubing.
 Conversely, at low production rates, significant heat

Table 4: Bottom hole pressure of gas well WELL 1X with different Temperature profiles.

Model	Pressure, psi
General temperature model	5083
Measured Data	5066
Linear Interpolation Temperature Data	4956
Software (Prosper)	4910

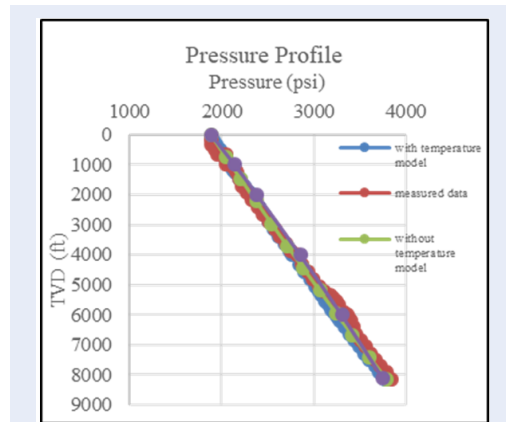


Figure 9: Pressure profile from 0 ft – 8100 ft

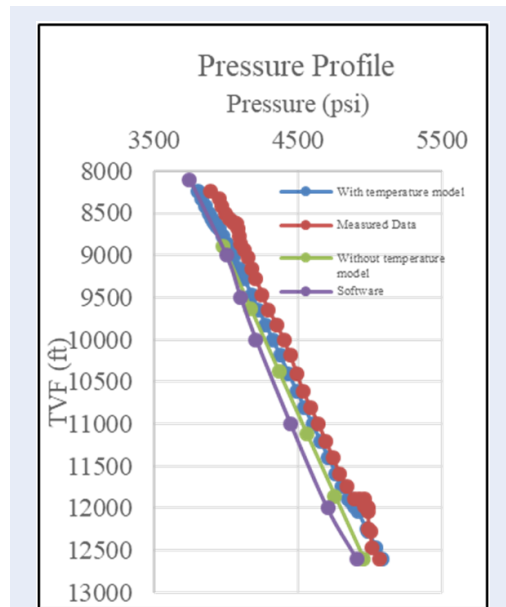


Figure 10: Pressure profile from 8100 ft – bottom hole

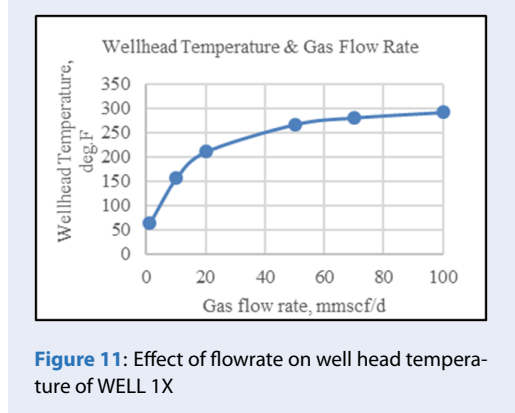


Figure 11: Effect of flowrate on well head temperature of WELL 1X

transfer to the surrounding environment results in a lower wellhead temperature. 328
329

Effect of tubing size on the temperature 330

It is imperative to acknowledge that alterations in tubing size can induce variations in the operating production. Consequently, for a comprehensive analysis, the study is conducted considering changes in tubing size while maintaining fixed operating production, as well as exploring diverse scenarios with varying operating production rates.. 331
332
333
334
335
336
337

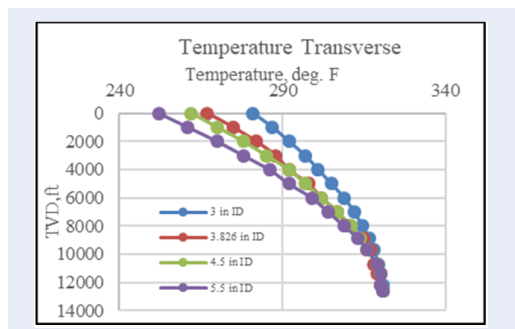


Figure 12: Effect of tubing size on well head temperature of WELL 1X

The impact of distinct tubing sizes is illustrated in Figure 12. The adjustment of tubing size leads to vari- 338
339

ations in both pressure and temperature at the wellhead. In general, as the tubing size increases, there is a substantial rise in wellhead pressure, coupled with a marginal decrease in wellhead temperature. Consequently, the inference drawn from this illustration is that tubing size exerts a considerable influence on wellhead pressure, with a comparatively minor effect on wellhead temperature.

Various Operating Production

Augmenting the tubing size facilitates an enhancement in the flow rate at the operating point, thereby resulting in increased production at the surface. In these instances, the node is situated at the wellhead location to scrutinize the ramifications of diverse operating conditions.

Figure 13 shows difference results from nodal analysis using with and without temperature models for determining the flow rate at bottom. In comparison to alternative models, the omission of a temperature model in the pressure calculation culminates in lower gas flow rates, particularly at 38 mmSCF/d and 49.51 mmSCF/d, as delineated in Table 5. This underscores the significance of integrating temperature considerations into the pressure model. The oversight of temperature effects along the tubing leads to a reduction in the produced gas flow rate.

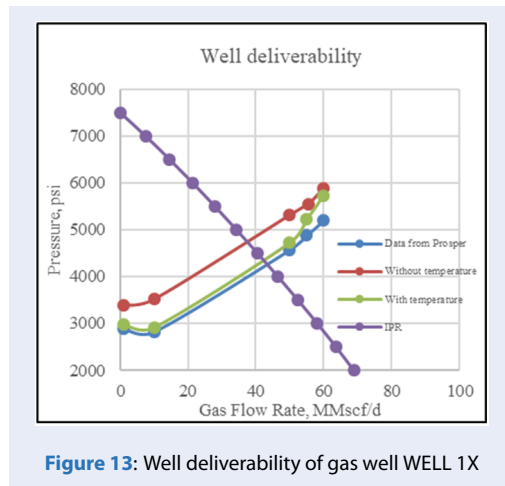


Figure 13: Well deliverability of gas well WELL 1X

CONCLUSION

This study introduces a model for predicting fluid flow temperature in oil wells, integrating the mechanical energy balance equation with three modes of heat transfer: convection, conduction, and radiation. The pressure calculation process incorporates the Gray correlation.

Key Findings:

The proposed model exhibits a negligible difference from the measured data, with a deviation of only 0.34% and 0.63% for pressure loss prediction and temperature distribution along the borehole, respectively. Nodal analysis emerges as a valuable technique for calculating pressure and temperature in the wellbore and reservoir flow, offering the capability for sensitivity analysis to assess the impact of various factors. Sensitivity analysis is conducted to evaluate the effects of tubing size and production rate on temperature and pressure in the wellbore, considering both the wellhead and bottom hole locations.

Conclusions from Sensitivity Analysis:

Changes in the flow rate exert a significant influence on the temperature along the production tubing. An increase in gas flow rate from 20 to 100 mmSCF/d results in a temperature rise from 150 to 300 °F.

Tubing size plays a pivotal role in pressure loss calculation. For a fixed production rate, increasing the tubing size from 3 to 5.5 inches leads to a slight decrease in wellhead temperature from 281 to 252 °F. However, considering various operating production rates, changes in tubing diameter induce significant variations in temperature and pressure.

NOMENCLATURE

- length of each segment, ft
- g_c : conversion factor, 32.17 lbm·ft/(lbf·sec²)
- h_c : convective heat coefficient, Btu/(hr·ft²·°F)
- H_L : holdup liquid
- h_f : radiative heat coefficient, Btu/(hr·ft²·°F)
- t_D : dimensionless time
- U_{to} : Overall heat transfer coefficient, Btu/(hr·ft²·°F)
- $\bar{\rho}$: average mixture density, lb/ft³
- A: relaxation distance, ft
- C_p : Specific-heat capacity, Btu/lb·°F
- d: Inner tubing diameter, ft
- F: Friction factor
- $f(t)$: Transient heat conduction function
- g: gravitational acceleration, ft/sec²
- Gr: Grashof number
- J: conversion factor for the mechanical equivalent of heat, ft·lbf/Btu
- k: thermal conductivity
- Nu: Nusselt number
- P: pressure, psi
- Pr: prandtl number
- r: radial distance or radius, ft
- Re: Reynold number
- T: temperature, °F
- v: velocity, ft/sec
- w: mass rate, lb/ft³

Table 5: Operation point with different prediction method

	BHP, psi	Q _g , mmscf/d
Without temperature model	4789	38
With temperature model	4289	49
Prosper	4223	51

425 β : fluid thermal expansion coefficient, 1/^oF

426 ϵ : emissivity

427 η : Joule-Thomson coefficient, ^oF·ft²/lbf

428 θ : inclination angle

429 σ : Stefan-Boltzmann constant, 1.731x10⁻⁹

430 Btu/(hr·ft²·^oR⁻⁴)

431 ϕ : lumped parameter, ^oF/ft

432 q: flow rate, stb/day

433 SUBSCRIPTS

434 an: annulus

435 f: fluid

436 to: outer tubing

437 ti: inner tubing

438 ci: inner casing

439 co: outer casing

440 ca: casing

441 t: tubing

442 wh: wellhead

443 wf: bottom hole

444 L: liquid

445 fri: friction

446 acc: acceleration

447 ele: elevation

448 CONFLICT OF INTEREST

449 The authors pledge the content is the results of re-
450 search of the authors. The figures and results in the
451 paper are true and of no competing interest.

452 AUTHORS' CONTRIBUTION

453 Ta Quoc Dung: Led the development of a novel model
454 for predicting fluid flow temperature in oil wells.

455 Do Duc Anh: Integrated the mechanical energy bal-
456 ance equation with convection, conduction, and ra-
457 diation for heat transfer, and incorporated the Gray
458 correlation for pressure calculation.

459 REFERENCES

460 1. Alves IN, Alhanati FJS, Shoham O. A Unified Model for Predicting
461 Flowing Temperature Distribution in Wellbores and Pipe-lines.
462 SPE Pron Eng. 1992;7:363-7; Available from: <https://doi.org/10.2118/20632-PA>.
463

2. Petroleum E. PROSPER Single Well Systems Analysis. 8th ed. 464
Scotland: Petroleum Experts; 2003; 465
3. Mach JPE, BK. A Nodal Approach for Applying Systems Analysis 466
to the Flowing and Artificial Lift Oil or Gas Well. 1979; 467
4. Phu NT, Hoanh NV, Dung TQ, Ha LT. Assessing the effect 468
of gas temperature on gas well performance. PetroVietNam 469
J. 2022;6; Available from: <https://doi.org/10.47800/PVJ.2022.06-06>. 470
5. Hasan AR, Kabir CS. Heat Transfer During Two-Phase Flow in 472
Wellbores; Part I-Formation Temperature. SPE Annual Techni- 473
cal Conference; 1991; Available from: <https://doi.org/10.2523/22866-MS>. 474
6. Willhite G. Over-all heat transfer coefficients in steam and 476
hot water injection wells. J Pet Technol. 1967;607-15; Available 477
from: <https://doi.org/10.2118/1449-PA>. 478
7. Sagar. Predicting Temperature Profiles in a Flowing Well. 479
1991; Available from: <https://doi.org/10.2118/19702-PA>. 480
8. Beggs H. Production Optimization Using Nodal Analysis. OGCI; 481
2003; 482
9. Tek MR. Temperature and Pressure Gradients In Gas Wells. 483
1978; Available from: <https://doi.org/10.2118/7495-MS>. 484

Đánh giá và phân tích ảnh hưởng của nhiệt độ trong khai thác khí tại Việt Nam

Tạ Quốc Dũng^{1,2,*}, Đỗ Đức Anh¹



Use your smartphone to scan this QR code and download this article

TÓM TẮT

Nghiên cứu đưa ra một mô hình toàn diện để dự đoán nhiệt độ của chất lỏng trong giếng khí, bằng cách tích hợp phương trình cân bằng năng lượng cơ học với các cơ chế truyền nhiệt thông qua khuếch tán, truyền dẫn và bức xạ. Tính toán áp suất được chính xác hóa bằng việc tích hợp hệ số tương quan Gray. Kết quả chính của nghiên cứu cho thấy độ chính xác hơn giữa mô hình đề xuất và dữ liệu đo lường, với sai số là 0.34% và 0.63% cho dự đoán tổn thất áp suất và phân bố nhiệt độ dọc theo giếng. Nghiên cứu đã sử dụng phân tích điểm nút là một công cụ hiệu quả để tính toán chính xác áp suất và nhiệt độ trong giếng và dòng chảy trong ống khai thác. Ngoài ra, thông qua phân tích độ nhạy, nghiên cứu đánh giá tác động của các yếu tố khác nhau, như kích thước ống và lưu lượng khai thác lên nhiệt độ và áp suất trong giếng từ vị trí đầu giếng đến đáy giếng. Kết quả từ phân tích độ nhạy nhấn mạnh ảnh hưởng đáng kể của sự thay đổi lưu lượng đối với nhiệt độ dọc theo ống khai thác khi tăng lưu lượng từ 20 đến 100 mmscf/d dẫn đến sự tăng nhiệt độ từ 150 đến 300 độ F. Kích thước ống được xác định là một yếu tố quyết định trong việc tính toán tổn thất áp suất, cho thấy nhiệt độ đầu giếng giảm nhẹ từ 281 đến 252 độ F khi tăng kích thước ống từ 3 đến 5.5 inch. Như vậy, đường kính ống khai thác khác nhau tạo ra các thay đổi đáng kể đối với nhiệt độ và áp suất với lưu lượng khai thác khác nhau.

Từ khóa: Nhiệt độ chất lưu, áp suất chất lưu, phân tích điểm nút, mô hình nhiệt độ, hiệu suất khai thác

¹Khoa Địa chất và Dầu khí, Trường Đại học Bách Khoa, Việt Nam

²Đại học Quốc gia Thành phố Hồ Chí Minh, Việt Nam

Liên hệ

Tạ Quốc Dũng, Khoa Địa chất và Dầu khí, Trường Đại học Bách Khoa, Việt Nam

Đại học Quốc gia Thành phố Hồ Chí Minh, Việt Nam

Email: tqdung@hcmut.edu.vn

Lịch sử

- Ngày nhận: 18-10-2023
- Ngày chấp nhận: 05-3-2024
- Ngày đăng:

DOI:



Bản quyền

© ĐHQG Tp.HCM. Đây là bài báo công bố mở được phát hành theo các điều khoản của the Creative Commons Attribution 4.0 International license.



Trích dẫn bài báo này: Dũng T Q, Anh D D. **Đánh giá và phân tích ảnh hưởng của nhiệt độ trong khai thác khí tại Việt Nam.** *Sci. Tech. Dev. J. - Eng. Tech.* 2024; ():1-1.